Acknowledgment. This research was supported by a contract, No. N01-AM-0-2208, from the National Institute of Arthritis, Diabetes, and Digestive and Kidney Diseases, U.S. Public Health Service.

Registry No. **3**, 98902-95-5; **4**, 112-26-5; **5**, 31255-11-5; **6**, 929-59-9; **7**, 59945-35-6; **8**, 98902-85-3; **9**, 98902-86-4; **10**, 98902-87-5; **11**, 98902-88-6; **12**, 98902-89-7; **14**, 98902-90-0; **15**, 19249-03-7; **16**, 98902-91-1; **17**, 98902-92-2; **18**, 98902-93-3; **18**·HCl, 98902-94-4; BSA, 10416-58-7; MoO_5, 12163-73-4; Fe^{3+}, 20074-52-6; $PhCH_2ONH_2$, 622-33-3; $BrCH_2CO_2H$, 79-08-3; potassium phthalimide, 1074-82-4; methyl acrylate, 96-33-3.

Contribution from the Department of Chemistry, Purdue University, West Lafayette, Indiana 47907

Substitution and Rearrangement Reactions of Nickel(III) Peptide Complexes in Acid

EDWARD J. SUBAK, JR., VINCENT M. LOYOLA, and DALE W. MARGERUM*

Received July 31, 1985

The terminal N(peptide) bonds to nickel in complexes of tetraglycine, $Ni^{III}(H_{-3}G_4)(H_2O)_2^-$, and tetraglycinamide, $Ni^{III}(H_{-3}G_4a)(H_2O)_2$, break rapidly in acid with first-order rate constants that range from 0.1 to 15 s^{-1} as the hydrogen ion concentration increases (0.004–1.0 M). However, the other three equatorial Ni(III)–N bonds are relatively inert to substitution. EPR spectra at room temperature and in frozen aqueous glasses help to characterize several protonated species for these complexes and for nickel(III) tripeptide complexes. The substitution reactions of the terminal peptide nitrogen in the Ni(III) complexes of G_4 and G_4a are reversible in dilute acid, and the nitrogen coordinates to the metal once again in the process of freezing the aqueous solutions for EPR measurements. The ternary complexes $Ni^{III}(H_{-2}peptide)(phen)(H_2O)$ and $Ni^{III}(H_{-2}peptide)(terpy)$ form readily in dilute acid with phen chelated to an axial and an equatorial site and with terpy coordinated to two axial sites and one equatorial site of nickel(III).

Introduction

Chemical or electrochemical oxidation of nickel(II) peptides yields nickel(III) complexes that have been characterized by electron paramagnetic resonance (EPR) and ultraviolet–visible spectroscopy as well as by cyclic voltammetry.[1-4] The UV–vis spectra of these Ni(III) species have two ligand-to-metal charge-transfer bands, one between 325 and 360 nm ($\epsilon \sim 5000$ M^{-1} cm^{-1}) and the other between 230 and 260 nm ($\epsilon \sim 11\,000$ M^{-1} cm^{-1}). The reduction potentials of the Ni(III,II) peptide couples fall in the range of 0.79–0.96 V (vs. NHE)[2] and vary less with the nature of the coordinated equatorial donors than is the case for the Cu(III,II) peptides.[5] Temperature-dependent electrode potential studies indicate that two coordinated water molecules are released when Ni(III) peptides are reduced to Ni(II) peptides.[4] EPR spectra (−150 °C) of frozen aqueous glasses of Ni(III) peptide solutions show that the metal is located in a tetragonally distorted octahedral environment and that the unpaired electron resides in a molecular orbital that has a large amount of d_{z^2} character.[3,6] Structures IA–C give the proposed

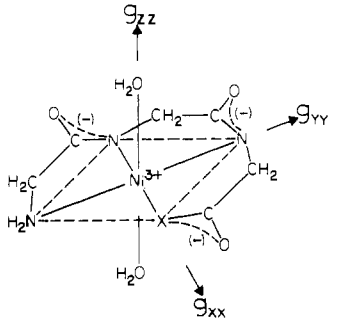

IA, $Ni^{III}(H_{-2}G_3)$, X = O
B, $Ni^{III}(H_{-3}G_4)^-$, X = NCH_2COO^-
C, $Ni^{III}(H_{-3}G_4a)$, X = NCH_2CONH_2

coordination geometry for $Ni^{III}(H_{-2}G_3)(H_2O)_2$, $Ni^{III}(H_{-3}G_4)(H_2O)_2^-$, and $Ni^{III}(H_{-3}G_4a)(H_2O)_2$, where G is the glycyl residue, a is an amide, and H_{-n} indicates n deprotonated peptide nitrogens. The x and y axes have different combinations of donor groups that contribute to a broad $g_\perp$ EPR signal and can be resolved into x and y components (g_{xx} and g_{yy}). In previous work[3] it has been shown that the magnitude of the equatorial g value increases as the strength of the equatorial donor increases in the order N^-(peptide) ≈ N^-(amide) > $-NH_2$ > imidazole ≈ CO_2^-.

In this work, the reactions of Ni(III) peptides with acid are examined in regard to EPR and UV–vis evidence for structural changes and for the kinetics of these changes. It also is shown that Ni(III) peptides readily form ternary complexes with terpy (2,2′:6′,2″-terpyridine) or phen (1,10-phenanthroline).

Experimental Section

Reagents. Triglycine (G_3), tri-L-alanine (A_3), L-alanylglycylglycine (AG_2), glycyl-L-alanylglycine (GAG), triglycinamide (G_3a), tetraglycine (G_4), and tetraglycinamide (G_4a) were obtained from Biosynthetika or Vega Fox. The purity of the peptides was confirmed by chromatographic analysis and by elemental analysis. Nickel perchlorate, prepared from nickel carbonate and perchloric acid, was recrystallized, and a stock solution was standardized by EDTA titration to a murexide end point. Sodium perchlorate solution, prepared from sodium carbonate and perchloric acid, was boiled to remove carbon dioxide and was standardized gravimetrically. Oxone ($2KHSO_5 \cdot KHSO_4 \cdot K_2SO_4$ from E. I. du Pont de Nemours & Co.) was used for rapid chemical oxidation to give nickel(III) complexes. Buffer solutions (0.050 ± 0.003 M) with an ionic strength of 0.1, adjusted with $NaClO_4$, were prepared from $ClCH_2CO$-OH for pH 2.4–3.6, CH_3COONa for pH 3.9–5.1, and NaH_2PO_4 above pH 6.3.

Nickel(II) peptide complexes were prepared in solution by the reaction of nickel perchlorate with excess peptide. (The excess was 2% for G_4a, 5% for G_4, 20% for G_3a, and 30% for the tripeptides.) This prevented the precipitation of $Ni(OH)_2$ when the pH of the solutions was adjusted to 10.5 by slow addition of NaOH solution, controlled by a Radiometer Model ABU 13 pH stat.

Equipment and Procedures. Nickel(III) peptide samples were prepared electrochemically by passing the corresponding Ni(II) peptide solution through a graphite powder working electrode that was packed in a porous-glass column and wrapped with a platinum-wire auxilary electrode.[7] Generally, the fully deprotonated form of the Ni(II) peptide complex (pH 10.5) was oxidized at a potential 200 mV more positive than the $E°$ value for the Ni(III,II) couple with flow rates below 1.5 mL min^{-1}. The accompanying electrolysis of water lowered the pH and the collected solution was adjusted immediately to the desired pH with buffers or standard acid solution, because the nickel(III) peptides un-

(1) Bossu, F. P.; Margerum, D. W. *J. Am. Chem. Soc.* **1976**, *98*, 4003–4004.
(2) Bossu, F. P.; Margerum, D. W. *Inorg. Chem.* **1977**, *16*, 1210–1214.
(3) Lappin, A. G.; Murray, C. K.; Margerum, D. W. *Inorg. Chem.* **1978**, *17*, 1630–1634.
(4) Youngblood, M. P.; Margerum, D. W. *Inorg. Chem.* **1980**, *19*, 3068–3072.
(5) Bossu, F. P.; Chellappa, K. L.; Margerum, D. W. *J. Am. Chem. Soc.* **1977**, *99*, 2195–2203.
(6) Sugiura, Y.; Mino, Y. *Inorg. Chem.* **1979**, *18*, 1336–1339.
(7) Clark, B. R.; Evans, D. H. *J. Electroanal. Chem. Interfacial Electronchem.* **1976**, *69*, 181–194.

0020-1669/85/1324-4350$01.50/0

Table I. Anisotropic g Values for Nickel(III)–Triglycine Complexes in Frozen Aqueous Perchloric Acid Glasses at −150 °C

−log [H⁺][a]	species type[b]	g_{xx}	g_{yy}	g_{zz}	g_{av}[c]
6.0	IA	2.242	2.295	2.015	2.184
3.51	IA	2.243	2.296	2.013	2.184
3.05	IA	2.243	2.296	2.013	2.184
2.54	IA	2.238	2.291	2.013	2.181
2.01	IVA	2.227	2.273	2.014	2.171
1.46	IVA	2.224	2.262	2.018	2.168
1.04	IVA	2.222	2.262	2.018	2.167
0.10[d]	IVA	2.212	2.249	2.017	2.160
−0.08[e]	IVA	2.218	2.258	2.020	2.165

[a] Acidity at room temperature before freezing. [b] See structures in Figure 2. [c] g_{av} is calculated from the g_{xx}, g_{yy}, and g_{zz} values. [d] 0.80 M $HClO_4$. [e] 1.20 M $HClO_4$.

dergo rapid redox decomposition at higher pH. The minimum time to prepare a sample for an EPR spectrum was about 200 s.

Chemical generation of Ni(III) peptides required only a few seconds and was used when their redox decomposition was rapid. Equal volumes of the monopersulfate solution and of nickel(II) peptide were mixed in a two-syringe push-flow mixer and plunged into a stirred buffer or perchloric acid solution. Aliquots were transferred to an EPR tube and placed in liquid nitrogen. The transfer/quench steps usually required 8–10 s.

The EPR spectra of magnetically dilute aqueous glasses that contained less than 8×10^{-4} M Ni(III) were measured at −150 ± 5 °C with a Varian Model E-109 X-band spectrometer modulated at 100 kHz and equipped with a Model E-238 variable-temperature cavity. The frozen $HClO_4/NaClO_4$ solutions gave adequate glasses, and no other solvents were added in their preparation. Magnetic field values were calibrated with reference to DPPH (α,α'-diphenyl-β-picrylhydrazyl).[8] The g values were obtained by matching the experimental spectra with computer-generated spectra.[3] Gaussian line shapes and broadening parameters, W, were used in the computed spectra. The W_{xx} and W_{yy} values were in the range 1.7–7.0 and 1.7–4.1, respectively, relative to unity for W_{zz}. The precision of the best fit g_{zz} values is ±0.003, while that of g_{xx} and g_{yy} is usually ±0.005.

Room-temperature EPR spectra were obtained with a Varian E-231 cavity. A thin cell (Wilmad WG-812) of 0.1-mm sample thickness was used to minimize microwave absorption by the water. Preliminary stopped-flow EPR measurements used a similar cell equipped with a two-jet mixer (Wilmad WG-804). When the flow stopped, a microswitch closed that actuated digital collection (Biomation Model 8100 transient recorder) of a 100 G wide spectrum. The magnetic field sweeps were generated with a Varian Model E-271A rapid-scan accessory and a Wavetech triangular waveform generator. These spectra were stored on a Tektronix Model 603 storage monitor.

Ultraviolet–visible spectra were obtained with a thermostated Cary Model 14. Molar absorptivities (ϵ) of the Ni(III) peptide complexes were measured with a precision of ±5% by spectrophotometric titrations with ascorbic acid as a reductant. Circular dichroism spectra of Ni(III) species that contained L-alanyl residues were measured with a Cary Model 61 CD spectrometer.

The kinetics of the Ni(III) peptide reactions in acid were followed by a vidicon stopped-flow spectrophotometer[9] to observe spectral changes. A Durrum stopped-flow spectrophotometer was used to measure rate constants at 25.0 ± 0.2 °C and an ionic strength of 1.0 M ($NaClO_4$).

Orion Model 601 and Instrumentation Laboratories Model 245 pH meters were used. The measured pH values were converted to −log [H⁺] by titration calibrations of standard perchloric acid and sodium hydroxide solutions at each ionic strength condition.

Results and Discussion

Tripeptide Nickel(III) Complexes. The EPR spectrum of an aqueous glassy sample of $Ni^{III}(H_{-2}G_3)(H_2O)_2$, frozen from a solution initially at pH 6, shows that the metal ion is in a tetragonally elongated octahedral environment with water molecules in the axial positions (along the elongated z axis). The resolved g values (Table I) are essentially constant when the initial solution pH is 3–6. However, as the solution pH is adjusted to 2 and lower, the g_{zz} value shifts slightly from 2.013 ± 0.002 to 2.017 ± 0.002,

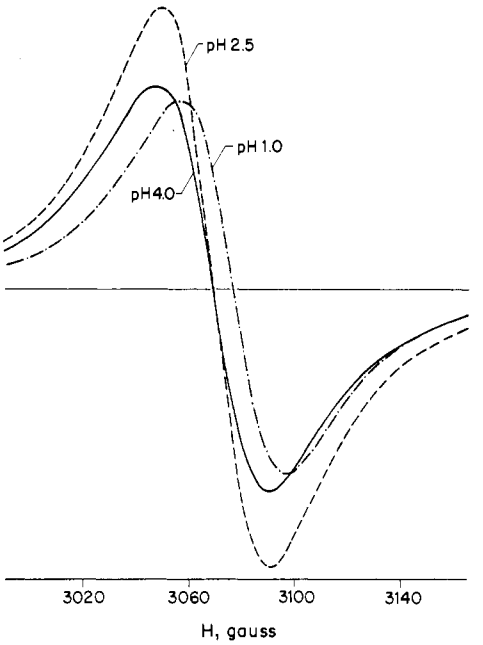

Figure 1. EPR spectral shifts (25 °C) for $Ni^{III}AG_2$ as the solution pH changes: —, pH 4.0; - - -, pH 2.5; –·–, pH 1.0.

Table II. UV–Visible Absorption Bands of Nickel(III)–Peptide Complexes in Acid at 25.0 °C

	λ_{max}, nm			
−log [H⁺]	G_3	G_3a	G_4	G_4a
6.5–4.0	340, 250	325, 235 sh	325, 240 sh	328, 240 sh
3.02	342, 240 sh	350, 250 sh	340, 260 sh	332, ~240
2.50	343, 250 sh	353, 250 sh	346, 260	340, ~240
2.46	340, 250			340, 243
1.94	340, 250			355, 245
1.38	342, 252			358, 246
1.00		360, 252		365, 250
0.92		360, 250	~345	
0.85	343, 250			

Table III. Molar Absorptivities of Selected Nickel(III)–Peptide Complexes in Acid

peptide	λ_{max}, nm	−log [H⁺]	ϵ, M^{-1} cm^{-1}
AG_2	350	4.00–0.82	4100 ± 150
A_3	340	6.50–1.00	4000 ± 100
GAG	340	4.00	4400 ± 200
G_4a	330	7.00	5500 ± 200
	300	5.00	5700 ± 200
	365	1.00	3500 ± 150

while the g_{xx} values (±0.004) decrease from 2.241 to 2.221 and the g_{yy} values (±0.004) decrease from 2.295 to 2.261. These changes correspond to weaker equatorial donors around nickel(III). The g_{av} value, equal to $^1/_3(g_{xx} + g_{yy} + g_{zz})$, also shifts significantly from 2.184 at pH 6 to 2.165 in 1.2 M $HClO_4$. Similar changes are found in the EPR spectra of other tripeptide complexes that contain L-alanyl residues (AG_2, GAG, A_3). The room-temperature EPR also change with pH as seen in Figure 1 for the AG_2 complex of nickel(III), where the isotropic g value, g_{iso}, shifts from 2.195 at pH 4.0 to 2.188 at pH 1.0. At an intermediate pH of 2.5 the EPR spectrum shifts only about 5 G, which indicates that the major change in the nickel(III) species occurs below pH 2.5. The changes in the intensities of the signals are not significant as they depend upon the sample preparation and the cell position in the magnetic field. Also, there is appreciable decomposition of the nickel(III) peptide complexes to form nickel(II) and oxidized peptide fragments.

In contrast to the EPR spectral changes, the UV–vis spectral bands for the nickel(III) complexes of G_3, AG_2, and A_3 are essentially unchanged from pH 6.5 to 0.85 (Tables II and III). Similarly, the CD spectrum of the GAG complex of nickel(III)

(8) Alger, R. S. "Electron Paramagnetic Resonance Techniques and Applications"; Interscience: New York, 1968; p 25.
(9) Ridder, G. M.; Margerum, D. W. *Anal. Chem.* **1977**, *49*, 2098–2108.

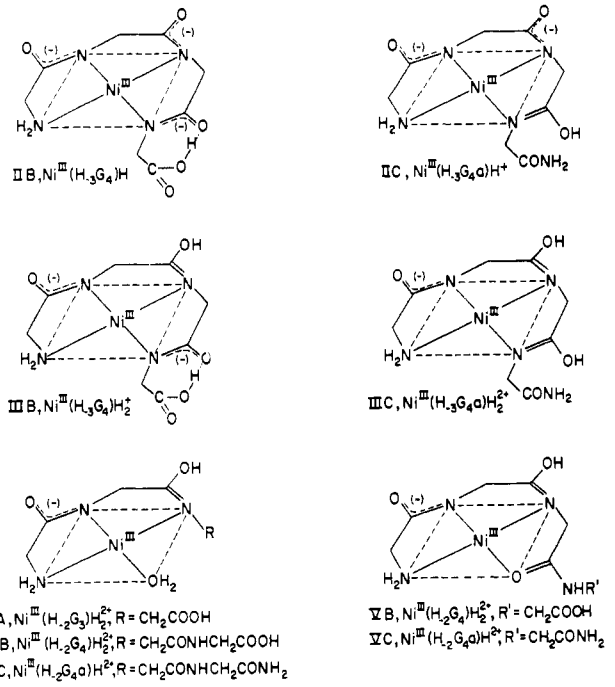

Figure 2. Proposed structures of protonated nickel(III) peptide complexes of G_3^-, G_4^-, and G_4a. All complexes have tetragonally elongated structures, but the two axial water molecules are omitted for simplicity.

undergoes no significant band shift between pH 7 and 0.4 M $HClO_4$. All the nickel(III) complexes decompose in aqueous solution, and above 0.01 M $[H^+]$ the rates of this decomposition increase. Although the UV–vis spectra do not indicate a change in the initial reactants as the acidity increases, the EPR spectra do show that some rapid protonation occurs. The changes are subtle and are consistent with the protonation of the carboxylate group and a peptide oxygen, rather than the protonation of a peptide nitrogen, which would cause larger EPR shifts and cause UV–vis changes.

The shift that acid causes in the g_{yy} values, as well as in the g_{xx} values, suggests that a peptide oxygen is protonated without loss of the metal–N(peptide) bond, as found in the crystal structure[10] of $Co^{III}(H_{-1}G_2)_2H_2^+$. This type of "outside protonation" has been postulated in a variety of kinetics studies in which metal peptide complexes rapidly add a proton prior to the cleavage of the metal–N(peptide) bond.[11-16] In these cases the protonation also occurs below pH 2.5. The proposed species for the triglycine complex at pH 2 or less is $[Ni^{III}(H_{-2}G_3)H_2]^{2+}$, as shown in structure IVA (Figure 2), where a peptide oxygen and the carboxylate group are protonated. An alternative structure would be $[Ni^{III}(H_{-2}G_3)H]^+$ where the carboxylate group remains coordinated. The EPR results give direct spectral evidence for the rapid addition of protons that weaken the equatorial bonding to nickel(III) and shift both the g_{xx} and g_{yy} values. Subsequent reactions of the nickel(III) tripeptide complexes with acid lead to redox decomposition.[17]

Nickel(III) Complexes of G_4 and G_4a. The nickel(II) complex of G_4 is square planar with the terminal amine and three deprotonated peptide nitrogens coordinated, as shown by the crystal

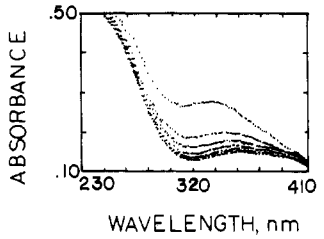

Figure 3. Stopped-flow rapid-scan UV–vis spectral changes in the reaction of $Ni^{III}(H_{-3}G_4a)$ with dilute $HClO_4$ ($[H^+]$ = 0.052 M, 25.0 °C, μ = 1.0 M). Absorbance (2-cm cell) decreases with time for spectra recorded at 0.02, 0.09, 0.16, 0.23, 0.30, 0.37, 0.42, and 0.49 s.

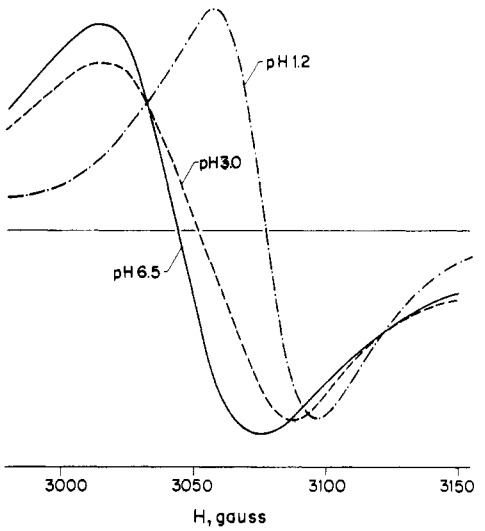

Figure 4. EPR spectral shifts (25 °C) for the $Ni^{III}G_4a$ complex as the solution pH changes: —, pH 6.5; - - -, pH 3.0; -·-, pH 1.2.

structure[18] of $Ni^{II}(H_{-3}G_4)^{2-}$. The reversibility[2] and the reaction entropies[4] of the nickel(III,II) redox couple as well as the EPR spectrum[3] indicate that the equatorial coordination of the nickel(III) complex is the same as that for the nickel(II) complex but that two water molecules are coordinated axially to give $Ni^{III}(H_{-3}G_4)(H_2O)_2^-$ (structure IB). The EPR spectrum of the G_4a complex shows that it has a similar geometry and forms $Ni^{III}(H_{-3}G_4a)(H_2O)_2$ (structure IC).

In contrast to the nickel(III) tripeptide complexes, the UV–vis spectra of the nickel(III) complexes of G_4, G_4a, and G_3a change as the pH is lowered (Tables II and III). The absorption bands for the G_4 complex shift about 20 nm to longer wavelengths between pH 6.5 and 2.5 and do not change significantly at lower pH. For $Ni^{III}(H_{-3}G_4a)$, one absorption band shifts 35 nm (from 330 nm at pH 7.0 to 365 nm at pH 1.0). A large decrease in the molar absorptivity accompanies the shift in the absorption maximum (Table III). The other absorption band shifts only 10 nm (240 nm at pH 7.0 to 250 nm at pH 1.0). The absorption spectra obtained with a vidicon stopped-flow spectrometer[9,19] (Figure 3) after mixing $Ni^{III}(H_{-3}G_4a)$ with dilute acid show that the shift in λ_{max} from 330 to 365 is a moderately fast process with a first-order rate constant of 1.54 s^{-1} at 25.0 °C in 0.052 M $HClO_4$. The protonation of peptide oxygens to form outside protonated complexes do not cause appreciable spectral shifts and are much more rapid reactions.[11-16] Hence, these results suggest that the spectral change observed is due to cleavage of the nickel(III)–N(peptide) bond and protonation of the peptide nitrogen.

The room-temperature EPR spectrum of the nickel(III)–G_4a complex has a 40-G shift as the pH is lowered as seen in Figure 4. The g_{iso} value for the G_4a complex changes from 2.220 (pH 6.5) to 2.210 (pH 3.0) and to 2.189 (pH 1.2). The last value is

(10) Barnet, M. T.; Freeman, H. C.; Buckingham, D. A.; Hsu, I.; van der Helm, D. *J. Chem. Soc. D* **1970**, 367–368.
(11) Paniago, E. B.; Margerum, D. W. *J. Am. Chem. Soc.* **1972**, *94*, 6704–6710.
(12) Wong, L. F.; Cooper, J. C.; Margerum, D. W. *J. Am. Chem. Soc.* **1976**, *98*, 7268–7274.
(13) Cooper, J. C.; Wong, L. F.; Margerum, D. W. *Inorg. Chem.* **1978**, *17*, 261–266.
(14) Raycheba, J. M. T.; Margerum, D. W. *Inorg. Chem.* **1980**, *19*, 497–500.
(15) Rybka, J. S.; Kurtz, J. L.; Neubecker, T. A.; Margerum, D. W. *Inorg. Chem.* **1980**, *19*, 2791–2796.
(16) Bannister, C. E.; Margerum, D. W. *Inorg. Chem.* **1981**, *20*, 3149–3155.
(17) Loyola, V. M.; Subak, E. J., Jr.; Margerum, D. W., to be submitted for publication.
(18) Freeman, H. C.; Guss, J. M.; Sinclair, R. L. *Chem. Commun.* **1968**, 485–487.
(19) Milano, M. J.; Pardue, H. L.; Cook, T. E.; Santini, R. E.; Margerum, D. W.; Raycheba, J. M. T. *Anal. Chem.* **1974**, *46*, 374–381.

Table IV. Anisotropic g Values as a Function of Acidity for the Ni^{III}–G_4 and Ni^{III}–G_4a Complexes in Frozen Aqueous Perchloric Acid Glass Samples at −150 °C

−log [H⁺][a]	species type[b]	g_{xx}	g_{yy}	g_{zz}	g_{av}[c]
	Peptide: G_4				
6.0	IB	2.297	2.278	2.010	2.195
4.25	IIB	2.298	2.267	2.014	2.193
3.30	IIB	2.297	2.266	2.014	2.192
3.00	IIB	2.298	2.260	2.012	2.190
2.50	IIIB	2.296	2.253	2.013	2.187
2.00	IIIB	2.293	2.249	2.013	2.185
1.00	IVB	2.230	2.268	2.016	2.171
0.74	IVB	2.236	2.270	2.018	2.175
0.10[d]	IVB	2.230	2.256	2.018	2.168
−0.08[e]	IVB	2.228	2.256	2.018	2.168
	Peptide: G_4a				
5.80	IC	2.308	2.282	2.012	2.201
4.70	IC	2.297	2.283	2.010	2.197
3.90	IC	2.308	2.283	2.013	2.197
2.85	IIC	2.244	2.284	2.017	2.182
2.48	IIIC	2.258	2.258	2.020	2.179
2.19	IIIC	2.255	2.255	2.020	2.177
1.90	IIIC	2.256	2.256	2.020	2.177
1.50	IIIC	2.256	2.256	2.018	2.175
1.01	IVC	2.237	2.267	2.018	2.174
0.54	IVC	2.232	2.266	2.018	2.172
0.28[f]	IVC	2.232	2.270	2.020	2.174
−0.20[g]	IVC	2.232	2.265	2.018	2.172

[a] Acidity at room temperature. [b] See structures in Figure 2. [c] g_{av} is $^1/_3(g_{xx} + g_{yy} + g_{zz})$. [d] 0.80 M $HClO_4$. [e] 1.20 M $HClO_4$. [f] 0.53 M $HClO_4$. [g] 1.60 M $HClO_4$.

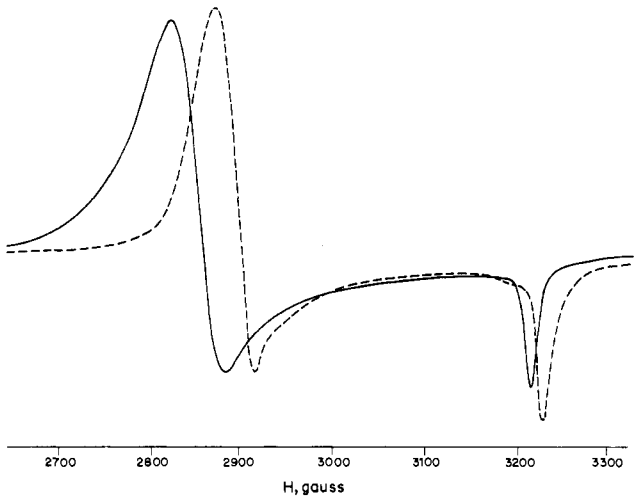

Figure 5. EPR spectra (9.078 GHz) in frozen aqueous glass (−150 °C) of $Ni^{III}G_4a$ prepared from solutions initially at pH 5.8 (—) and at pH 0.54 (---). The receiver gain was a factor of 2 larger for the pH 0.54 spectrum.

the same as that found for the nickel(III)–AG_2 complex at pH 1.0. These changes for G_4a are consistent with the replacement of the deprotonated peptide nitrogen from the fourth position (position X in structure IC) by a weaker donor, such as a peptide oxygen or a water molecule.

The frozen-solution EPR spectra of Ni(III)–G_4a change with the pH of the solutions prior to the freezing process. The best fit of the g values determined by spectral matching are summarized in Table IV. The value of g_{xx} undergoes the most dramatic change from 2.308 at pH 5.8 to 2.232 at pH 0.54. This amounts to a spectral shift of approximately 90 G as seen in Figure 5. The g_{yy} values also decrease as the acidity increases but to a lesser extent than for g_{xx}. On the other hand, the g_{zz} values show a small, yet a significant, increase as the acidity increases. The observed changes are consistent with weaker equatorial donor strength and stronger axial solvation. On the basis of the changes in the g values, four different Ni(III)–G_4a species are postulated as designated in Table IV. Species IC is the initial deprotonated complex that is present above pH 3. As the acidity is increased, the first significant change in the frozen-solution spectra occurs at −log [H⁺] = 2.85, where g_{xx} changes from 2.304 to 2.244, while g_{yy} remains constant and g_{zz} increases slightly. Protonation of a peptide oxygen as shown in structure IIC (Figure 2) is proposed to be responsible for this change. In the hydrogen ion concentration range of $10^{-2.48}$–$10^{-1.5}$, the g_{yy} values decrease to 2.256 and the g_{xx} values are the same. (In these spectra the g_{yy} and g_{xx} values cannot be resolved from one another.) Structure IIIC is proposed with a second peptide oxygen protonated but with all the nitrogens still coordinated. Finally, above 0.1 M $HClO_4$ the g_{xx} values decrease to 2.232 and structure IVC is proposed in which the fourth nitrogen is protonated and displaced from nickel(III). This equatorial position could be occupied by a coordinated water molecule or by a peptide oxygen (VC).

Table V. First-Order Rate Constants for the Substitution of the Fourth Nitrogen of G_4a and of G_4 in Their Nickel(III) Complexes

[H⁺], M	k_{obsd}, s^{-1}[a] Ni^{III}-($H_{-3}G_4a$)	k_{obsd}, s^{-1}[a] Ni^{III}-$(H_{-3}G_4)^-$	[H⁺], M	k_{obsd}, s^{-1}[a] Ni^{III}-($H_{-3}G_4a$)	k_{obsd}, s^{-1}[a] Ni^{III}-$(H_{-3}G_4)^-$
0.0043	0.142	1.50	0.254	5.55	11.8
0.0145	0.440	2.38	0.355	6.68	12.4
0.0520	1.51	5.93	0.501	7.96	13.8
0.0650	1.80	6.50	0.657	9.02	14.5
0.128	3.22	8.47	0.809	9.75	15.0
0.204	4.76		0.950	10.1	14.7

[a] Measured at 320 nm, 25.0 °C, 1.00 M ionic strength ($NaClO_4$), with a precision ±4%.

Changes in the frozen-solution EPR spectra of $Ni^{III}(H_{-3}G_4)^-$ in acid are not as gradual as those of the G_4a complex. The g_{xx} values show only one sharp break. Above pH 2 the average g_{xx} value is 2.297, while at pH 1 and below the average g_{xx} value is 2.231. This corresponds to a substantial shift of 80 G in the spectra. At low pH the average g_{yy} value is 2.263, so g_{xx} and g_{yy} are virtually the same as the values found for G_4a at low pH. Similar structures are proposed (IVB or VB). The g_{yy} values for G_4 undergo less substantial changes, and structures IIB and IIIB are suggested. We know from kinetics studies of $Ni^{II}(H_{-3}G_4)^{2-}$ and of $Cu^{III}(H_{-3}G_4)^-$ that the free carboxylate group has a protonation constant of $10^{4.1}$ M^{-1} for the Ni(II) complex[11] and $10^{4.3}$ M^{-1} for the Cu(III) complex.[15] These studies also indicate that the resulting carboxylic acid is hydrogen-bonded to the nearest peptide oxygen as shown in structure IIB. We propose that this internal hydrogen bonding makes it more difficult to further protonate the terminal peptide oxygen. Hence the g_{xx} value is unchanged until 0.1 M acid is reached. However, below pH 2.5 the peptide oxygen in the third position appears to be protonated to give structure IIIB.

Kinetics of the Protonation Reactions of $Ni^{III}(H_{-3}G_4)^-$ and $Ni^{III}(H_{-3}G_4a)$. The loss of the fourth nitrogen from the coordination sphere of the Ni(III) complexes of G_4 and G_4a in dilute acid is readily measured by stopped-flow spectroscopy (Table V). The reaction rates are first order in the Ni(III) complex at all acidities and are also first order in hydrogen ion concentration at low acidities. In higher acid concentrations, the reactions of the G_4a complex become less than first order in hydrogen ion and for the G_4 complex the reactions nearly reach a zero-order dependence in hydrogen ion. A similar type of acid dependence has been observed for the dissociation reactions of Ni(II) complexes of G_4,[11] G_3a,[11,20] and G_4a.[14]

The proposed mechanism for the protonation and partial dissociation of $Ni^{III}(H_{-3}G_4a)$ is given in Figure 6. The observed pseudo-first-order rate constants in Table V are resolved in accord with eq 1, where K_1 (2.2 M^{-1}) is the equilibrium constant for the

$$k_{obsd} = K_1k_1[H^+]/(1 + K_1[H^+]) \quad (1)$$

rapid outside protonation step to give species IIC and k_1 (15.3

(20) Kupchunos, B.; Margerum, D. W., unpublished results.

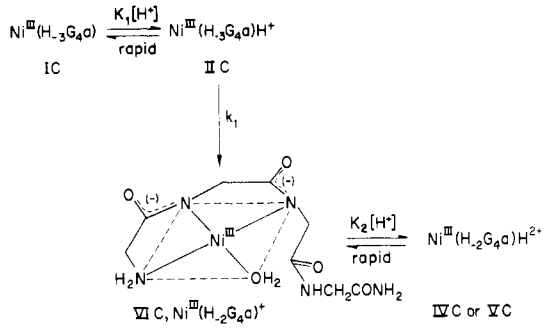

Figure 6. Proposed mechanism for the reaction of $Ni^{III}(H_{-3}G_4a)$ with acid. Rapid protonation of a peptide oxygen (K_1) is followed by the rate-determining step (k_1), where the peptide nitrogen is protonated and its bond to nickel(III) is broken to give VIC (axial waters are not shown). At low pH another proton adds rapidly to give IVC, and this species could rearrange to give VC.

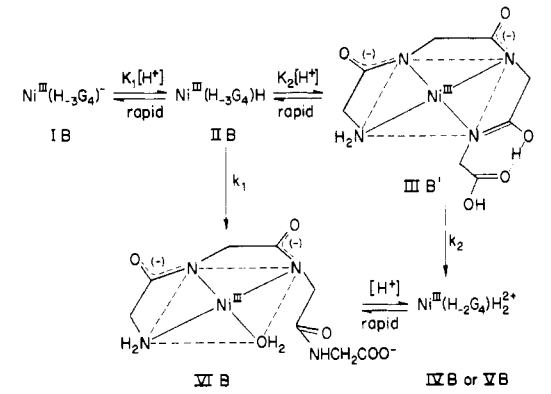

Figure 7. Proposed mechanism for the reaction of $Ni^{III}(H_{-3}G_4)^-$ with acid. Rapid protonation of the free carboxylate group (K_1) can lead to nickel(III)–N(peptide) bond cleavage (k_1), but additional protonation (K_2) of the terminal peptide oxygen to give IIIB′ leads to a more rapid loss of the terminal N(peptide) group from nickel. Axial waters are not shown.

s^{-1}) is the rate constant for the protonation of the peptide nitrogen and its cleavage from Ni(III) to give species VIC.

The proposed mechanism for the protonation and partial dissociation of $Ni^{III}(H_{-3}G_4)^-$ is given in Figure 7. Under the acid conditions used, species IB is fully converted to species IIB, $Ni^{III}(H_{-3}G_4)H$, where the carboxylate group is protonated. The K_1 value is expected to be about 10^4 M^{-1} from comparison with the corresponding Ni(II) and Cu(III) complexes. The kinetics data indicate that the value must be larger than $10^{3.6}$. The observed rate constants in Table V are resolved in accord with eq 2, where k_1 (0.9 s^{-1}) is the rate constant for the rearrangement

$$k_{obsd} = (k_1 + K_2k_2[H^+])/(1 + K_2[H^+]) \qquad (2)$$

of the outside protonated species IIB to the inside protonated species VIB. Another proton-assisted path exists with an equilibrium constant K_2 (8 M^{-1}) to form $Ni^{III}(H_{-3}G_4)H_2^+$, species IIIB′. The frozen-solution EPR data gave evidence for species IIIB, where the peptide oxygen on the second amino acid residue is protonated rather than the peptide oxygen on the third residue as shown in IIIB′. However, IIIB would not be expected to contribute as much as IIIB′ to the kinetic pathway where the adjacent fourth peptide nitrogen bond to nickel is cleaved with rate constant k_2 (17 s^{-1}). Figure 8 shows the fit of the resolved rate constants with the experimental dependence of k_{obsd} on $[H^+]$ for the protonation and rearrangement reactions of $Ni^{III}(H_{-3}G_4)^-$. The product of the reaction is IVB or VB, where either a water molecule or a peptide oxygen is coordinated to the fourth equatorial position of nickel(III).

No further protonation and unwrapping of G_4 or G_4a from Ni(III) can be observed prior to redox decomposition. Any subsequent acid dissociation reaction that might accompany the redox formation of Ni(II) is at least a factor of 10^3 slower. Thus,

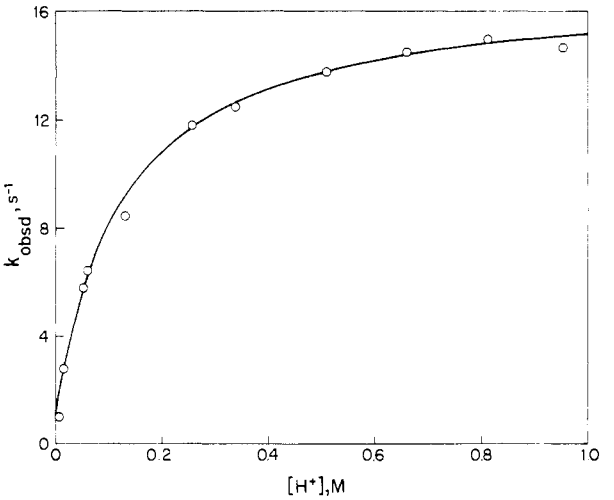

Figure 8. Hydrogen ion dependence of the observed pseudo-first-order rate constant (25.0 °C, μ = 1.0 M) for the rearrangement reaction of $Ni^{III}(H_{-3}G_4)^-$ to form $Ni^{III}(H_{-2}G_4)$ (VIB) and $Ni^{III}(H_{-2}G_4)H_2^{2+}$. The points are experimental, and the curve is calculated from eq 2.

Table VI. Summary of Kinetics Data (25.0 °C) for the Loss of the Fourth Nitrogen from Its Coordination to Nickel(III) Peptides[a] Compared to Data for Nickel(II) Peptides[b]

initial complex	k_0, s^{-1}	K_1, M^{-1}	k_1, s^{-1}	K_2, M^{-1}	k_2, s^{-1}
$Ni^{III}(H_{-3}G_4)^-$	$<10^{-4}$	$>10^{3.6}$	0.9 ± 0.5	8 ± 1	17 ± 3
$Ni^{III}(H_{-3}G_4a)$	$<2 \times 10^{-2}$	$10^{0.34}$	15.3 ± 0.7		
$Ni^{II}(H_{-3}G_4)^{2-}$	1.6×10^{-5}	$10^{4.2}$	5.6	~30	
$Ni^{II}(H_{-3}G_4a)^-$	8×10^{-5}	$10^{2.4}$	12	20	43
$Ni^{II}(H_{-3}G_3a)^-$	2×10^{-4}	$10^{2.6}$	208		

[a] This work, μ = 1.0 ($HClO_4$ and $NaClO_4$). [b] $Ni^{II}(H_{-3}G_4)^{2-}$, μ = 0.1 ($HClO_4$ and $NaClO_4$), ref 11; $Ni^{II}(H_{-3}G_4a)^-$, μ = 1.0 ($HClO_4$ and $NaClO_4$), ref 14; $Ni^{II}(H_{-3}G_3a)^-$, μ = 2.0 ($HClO_4$ and $NaClO_4$), ref 20.

the terminally coordinated peptide nitrogen is much more reactive than the remaining coordinated nitrogens.

A comparison of the corresponding reactions of $Ni^{II}(H_{-3}G_4)^{2-}$, $Ni^{II}(H_{-3}G_4a)^-$, and $Ni^{II}(H_{-3}G_3a)^-$ is given in Table VI. There are many similarities. The nickel(II) species have a water dissociation rate constant (k_0), but this pathway could not be measured for the nickel(III) species because of interference from redox reactions. The outside protonation constant, K_1, for $Ni^{II}(H_{-3}G_4a)^-$ is $10^{2.4}$, a factor of 100 larger than that for the corresponding protonation of $Ni^{III}(H_{-3}G_4a)$. On the other hand, the rate constants (k_1) for the dissociation step are remarkably similar to the values of 12 s^{-1} for the Ni(II) complex and 15 s^{-1} for the Ni(III) complex. The contrast in the rates of the subsequent dissociation steps is striking, because for Ni(II) the additional unwrapping reactions are rapid and the observed products are Ni_{aq}^{2+} and protonated peptides. The subsequent unwrapping steps of the peptides from Ni(III) are slow processes.

Reversibility of Unwrapping in the Freezing Process. One confusing aspect in our studies of these Ni(III) peptide complexes was the apparent discrepancy between room-temperature and frozen-solution structural assignments. The loss of one deprotonated peptide nitrogen from the Ni(III) complexes of G_4 and G_4a began near pH 2 as shown by UV–vis changes, by stopped-flow kinetics, and by room-temperature EPR shifts. Yet the frozen-glass EPR spectra of these solutions after the reactions had occurred in solution indicated that the peptide nitrogens were still coordinated. Furthermore, the frozen-solution EPR spectra indicated that peptide oxygens were more easily protonated (by 1 or 2 pH units) than the kinetics results showed. The reason for this behavior is that the reactions are reversible and the species present shift as the temperature is lowered and as the solution is frozen. For example, when the temperature of a solution of Ni(III)–G_4a in 0.023 M $HClO_4$ is increased from 8 to 23 °C, the EPR spectrum shifts approximately 7 G and the g_{iso} value changes from 2.194 to 2.188. Similarly, the absorption maximum of this

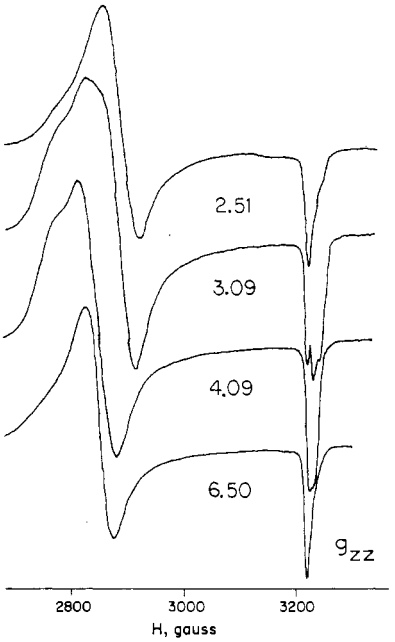

Figure 9. Frozen-solution EPR spectra (−150 °C) of $Ni^{III}G_4a$ in 0.05 M acetate buffer (pH 6.50 and 4.09) and in 0.05 M chloroacetate buffer (pH 3.09 and 2.51).

solution changes from 345 nm at 2.0 °C to 355 nm at 25.0 °C. These changes correspond to a lower degree of unwrapping at lower temperatures. Other work has shown that the freezing process itself can greatly increase the concentration of nickel(III) peptide axial adducts with chloride ion or with ammonia.[21] The axial coordination positions are extremely labile, and the equilibrium shifts greatly as the solution freezes. In this work, the solutions freeze in about 10 s. At intermediate pH values the composition of solutions change in regard to the labile equatorial position. This behavior is not found at higher pH where protonation has not taken place or at lower pH where it becomes difficult to reverse the reactions.

Mixed Species Observed in Frozen Buffer Solutions. The EPR spectra of Ni(III) peptides that are frozen from solutions buffered with 0.05 M acetic acid or chloroacetic acid indicate the presence of more than one species. Although acetate and chloroacetate complexation with Ni(III) peptides is negligible at room temperature,[21] this may not be the case for the frozen solutions. Figure 9 shows G_4a spectra obtained from acetate buffer (pH 6.50 and 4.09) and from chloroacetate buffer (pH 3.09 and 2.51). The g_{zz} splitting indicates the presence of two species at pH 4.09 and three species at pH 3.09. The buffer prevents some of the shift in equilibria observed when dilute $HClO_4$ solutions are frozen, so that more than one of the species IC–IVC may be present in the frozen sample. However, additional species also appear to be present because g_{zz} values of 2.001, 2.008, and 2.015 are found. At pH 2.5 both the G_4a and the G_4 complexes in the presence of chloroacetic acid give the same EPR spectrum with $g_{xx} = 2.26$, $g_{yy} = 2.27$, and $g_{zz} = 2.015$. This does not match spectra obtained from $HClO_4$ solutions and may be caused by a chloroacetic acid adduct as indicated in structure VII.

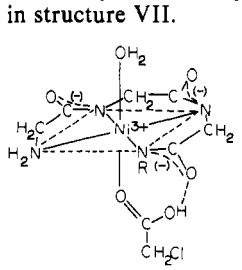

VII, $Ni^{III}(H_{-3}G_4a)(ClCH_2COOH)$, $R = CH_2CONH_2$

(21) Murray, C. K.; Margerum, D. W. *Inorg. Chem.* **1982**, *21*, 3501–3506.

Table VII. EPR Parameters for Frozen Aqueous Glass Samples at −150 °C of Nickel(III) Peptides with an Additional Ligand Coordinated

complex	g_{xx}	g_{yy}	g_{zz}	g_{zz} splitting	A_{zz}
$Ni^{III}(H_{-3}G_3a)(NH_3)$[a]	2.217	2.217	2.011	3	23.4
$Ni^{III}(H_{-3}G_3a)(NH_3)_2$[a]	2.178	2.178	2.019	5	19.0
$Ni^{III}(H_{-2}G_3a)(H_{-1}G_3a)$[a]	2.196	2.196	2.023	3	21.3
$Ni^{III}(H_{-2}G_3)$(phen)	2.174	2.206	2.017	3	22.0
$Ni^{III}(H_{-2}G_4)$(phen)	2.174	2.206	2.017	3	22.0
$Ni^{III}(H_{-2}G_3)$(terpy)	2.172	2.150	2.016	5	20.0
$Ni^{III}(H_{-2}G_3a)(terpy)^+$	2.172	2.150	2.016	5	20.0
$Ni^{III}(H_{-2}G_4)$(terpy)	2.172	2.150	2.016	5	20.0
$Ni^{III}(H_{-2}G_4a)(terpy)^+$	2.172	2.150	2.016	5	20.0

[a] Reference 3.

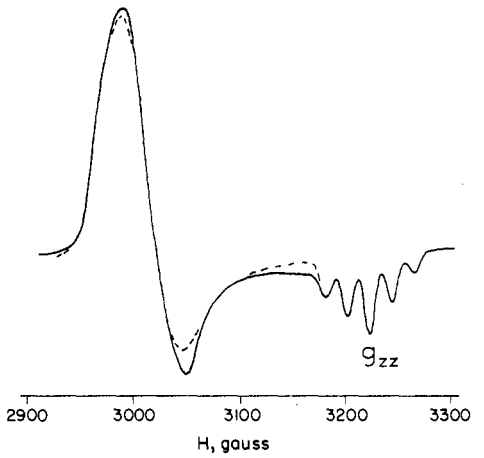

Figure 10. Frozen-solution EPR spectrum (−150 °C) of $[Ni^{III}(H_{-2}G_4a)(terpy)]^+$.

Ternary Complexes of Ni(III) Peptides with phen and terpy. Another demonstration of the relative lability of the fourth equatorial position of the Ni(III) peptides is the formation of ternary complexes with 1,10-phenanthroline and with 2,2′:6′,2″-terpyridyl. The Ni(III) complexes of G_3, G_3a, G_4, and G_4a form phen adducts that have one axial nitrogen and terpy adducts that have two axial nitrogens coordinated to the metal. The EPR parameters of these ternary species are given in Table VII together with the g values of the ammonia adducts[3] for comparison. The three-line g_{zz} splitting for phen indicates one axial nitrogen donor, while the five-line g_{zz} splitting for terpy indicates two equivalent axial nitrogen donors. Between pH 2.0 and 9.5, $Ni^{III}(H_{-2}G_3)$ adds phen (1×10^{-4} M) rapidly ($t_{1/2} < 0.1$ s). At room temperature the g_{iso} value shifts from 2.195 to 2.142 when phen adds, and there also is evidence of a 3-fold splitting with $A_{iso} \sim 15$ G. The frozen samples with the phen adduct give an A_{zz} value of 22.0 G, and the g_{xx} values decrease from 2.242 to 2.174, while the g_{yy} values decrease from 2.295 to 2.206. These data are consistent with bidentate coordination of phen with one nitrogen donor in an axial position and the other nitrogen donor in an equatorial position in place of the carboxylate oxygen at position X in structure IA.

At pH 5.0, $Ni^{III}(H_{-3}G_4)^-$ adds phen (1×10^{-4} M) somewhat slower ($t_{1/2} \sim 2$ s) than does the G_3 complex, but the resulting adduct has an identical EPR spectrum. At higher pH the reaction is much slower, while at lower pH the rate of addition of phen to the nickel(III)–G_4 complex is faster. This indicates that protonation of $Ni^{III}(H_{-3}G_4)^-$ facilitates the removal of the fourth peptide nitrogen and permits the formation of the $[Ni^{III}(H_{-2}G_4)(phen)]$ complex.

terpy also adds to several Ni(III) peptide complexes to give species with three terpy nitrogens and three peptide nitrogens bound to nickel. Figure 10 shows the frozen-solution EPR spectrum of the $[Ni^{III}(H_{-2}G_4a)(terpy)]^+$ complex. Structure VIII is proposed because identical EPR spectra are found for the terpy adducts with the Ni(III) complexes of G_3, G_3a, and G_4. The

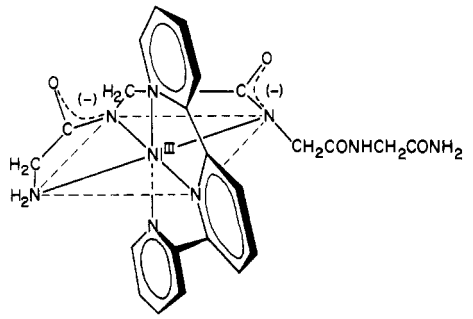

VIII, $[Ni^{III}(H_{-2}G_4a)(terpy)]^+$

splitting of g_{zz} into five peaks (A_{zz} = 20.0 G) shows two equivalent axial nitrogens are present. The equatorial plane is defined by the strongest donors, which are the amine nitrogen, two deprotonated peptide nitrogens, and one pyridyl nitrogen from terpy. The elongated axis has the two terminal pyridyl nitrogens from terpy. The g_{av} value decreases significantly to a value of only 2.113 for these terpy adducts.

Conclusions

Systematic changes in isotropic and anisotropic EPR spectra (and the corresponding **g** tensors) permit structural assignments to be made for nickel(III) peptide complexes as a function of acidity and in the presence of other chelating ligands. The substitution lability of the six coordination positions of nickel(III) differ greatly. Previous work[3,21] has shown that the elongated axial donors are extremely labile. This work shows that one of the equatorial positions is relatively labile. Carboxylate or peptide nitrogen groups coordinated in the fourth equatorial position (from the terminal amine of the peptide) undergo substitution and protonation reactions much more rapidly (by factors of 10^3 or more) than the other coordinated groups (an amine and two deprotonated peptide nitrogens). The changes in EPR spectra and the kinetics of the reactions in acid provide evidence for peptide oxygen protonation of the nickel(III) peptide complexes.

Acknowledgment. This work was supported by Public Health Service Grant No. GM-12152 from the National Institutes of General Medical Sciences. The assistance of Dr. George E. Kirvan in the preparation of the manuscript is appreciated.

Contribution from the Department of Chemistry, Purdue University, West Lafayette, Indiana 47907

Polypyridine and Polyamine Mixed-Ligand Complexes of Tripeptidonickel(III)

THOMAS L. PAPPENHAGEN, WILLIAM R. KENNEDY, CONRAD P. BOWERS, and DALE W. MARGERUM*

Received August 9, 1985

The GGG, GAG, and GGA tripeptide complexes of nickel(III) undergo substitution reactions with en, dien, bpy, phen, and terpy to form relatively stable chelated ternary complexes. Peptide complexes with Aib (α-aminoisobutyric acid) in the third residue are sterically hindered in the formation of chelate adducts. Thus, $Ni^{III}(H_{-2}Aib_3)(H_2O)_2$ does not form polypyridine adducts and forms only monodentate axially coordinated polyamine adducts. EPR spectra of frozen aqueous solutions show that the $Ni^{III}(H_{-2}GGA)$dien complex can exist in three forms. Dien is monodentate with axial Ni(III) coordination below pH 4, it is bidentate at pH 7–8 (the GGA carboxylate group is replaced to give five nitrogens coordinated to nickel), and it is tridentate above pH 11 to give the mixed complex with six coordinated nitrogens. $Ni^{III}(H_{-2}GAG)$terpy has six nitrogens coordinated to nickel(III) from pH 2 to pH 11. The stability constant for terpy addition is $10^{12.8}$ M^{-1}. This ternary complex has a reduction potential of 0.56 V (vs. NHE). Terpy also stabilizes the nickel(III) peptide complex in regard to self-redox decomposition reactions in basic solution.

Introduction

Nickel(III) peptide complexes have been characterized by their electrode potentials, EPR and UV–vis spectra, electron-transfer reactions, redox decomposition rates,[1-8] and, more recently EXAFS.[9] The *trans*-diaquanickel(III) tripeptide complexes (e.g. $Ni^{III}(H_{-2}GAG)(H_2O)_2$,[10] structure **1**) and tripeptide amide complexes undergo rapid substitution of axial water molecules to form 1:1 adducts with ammonia, imidazole, or pyridine.[6] These substituted nickel(III) peptide complexes are characterized by an increased kinetic stability to redox decomposition in neutral and basic solution and by a lowered reduction potential when compared

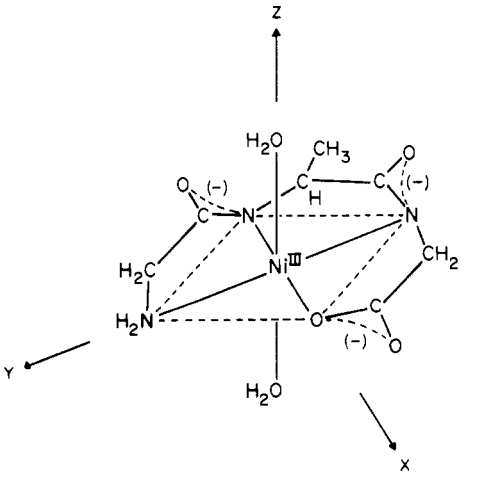

1

with that of the parent nickel(III) peptide complex.

Nickel(III) tris(diimine) complexes (e.g. $Ni(bpy)_3^{3+}$) have been formed in strongly acidic solution[11-13] and in acetonitrile.[14] These

(1) Bossu, F. P.; Margerum, D. W. *J. Am. Chem. Soc.* **1976**, *98*, 4003–4004.
(2) Bossu, F. P.; Margerum, D. W. *Inorg. Chem.* **1977**, *16*, 1210–1214.
(3) Lappin, A. G.; Murray, C. K.; Margerum, D. W. *Inorg. Chem.* **1978**, *17*, 1630–1634.
(4) Sugiura, Y.; Mino, Y. *Inorg. Chem.* **1979**, *18*, 1336–1339.
(5) Sakurai, T.; Hongo, J.; Nakahara, A.; Nakao, Y. *Inorg. Chim. Acta* **1980**, *46*, 205–210.
(6) Murray, C. K.; Margerum, D. W. *Inorg. Chem.* **1982**, *21*, 3501–3506.
(7) Jacobs, S. A.; Margerum, D. W. *Inorg. Chem.* **1984**, *23*, 1195–1201.
(8) Kirvan, G. E.; Margerum, D. W. *Inorg. Chem.* **1985**, *24*, 3245–3253.
(9) Kennedy, W. R.; Powell, D. R.; Niederhoffer, E. C.; Teo, B. K.; Orme-Johnson, W. H.; Margerum, D. W., to be submitted for publication.
(10) GAG is the tripeptide glycyl-L-alanylglycine and H_{-2} refers to the two deprotonated peptide nitrogens coordinated to nickel.
(11) Wells, C. F.; Fox, D. *J. Chem. Soc., Dalton Trans* **1977**, 1498–1501.

0020-1669/85/1324-4356$01.50/0